Deutsches Elektronen-Synchrotron

Summer Student Project

THz Beamline at FLASH

Authors:
Marija Šindik
Marina Nikolić

Supervisors :
Dr. Rui Pan
Dr. Sven Toleikis

September 7, 2018

Contents

1 Introduction

During our internship at Deutsches Elektronen-Synchrotron (DESY), we worked in the FLASH group, as part of the team that performs experiments on the terahertz beamline (BL3).

Our report covers 3 different topics. First, we were given the task of testing the stability of new compact models of mirror mounts, which if proven reliable could be used in THz-XUV pump-probe experiment. Second, we were entrusted with data analysis for the pump-probe experiment, which provided useful information for the scanning process during the experiment. And lastly, we managed to program the delay stage for 2D scanning of the sample in THz time-domain spectroscopy (TDS) system, which will hopefully prove useful in future experiments.

1.1 Free electron laser

A free electron laser (FEL) is a high-power tunable laser which consists of an electron beam traversing a slalom path through a periodic magnetic field. In conventional lasers, the electrons are bound to atoms or molecules and can only receive certain (discrete) amount of energy [1]. Therefore, the laser frequency is limited by the energy configuration of atoms and molecules. In FEL, the electrons are not in a bound state, they are "free", hence the name free electron laser. That is what makes FELs tunable over a wide range of frequencies – from microwave, terahertz and infrared to visible light, ultraviolet (UV), extreme ultraviolet (XUV) all the way to X rays. In order to achieve such wide spectral range, FELs use a large-scale particle accelerator to produce the high quality and high-energy electron beams. A periodic magnetic field is realized in the so-called undulators, which are a periodic structure of dipole magnets with alternating polarity. The laser frequency can be adjusted by controlling the energy of the electrons in the accelerator, or by modifying the magnetic fields.

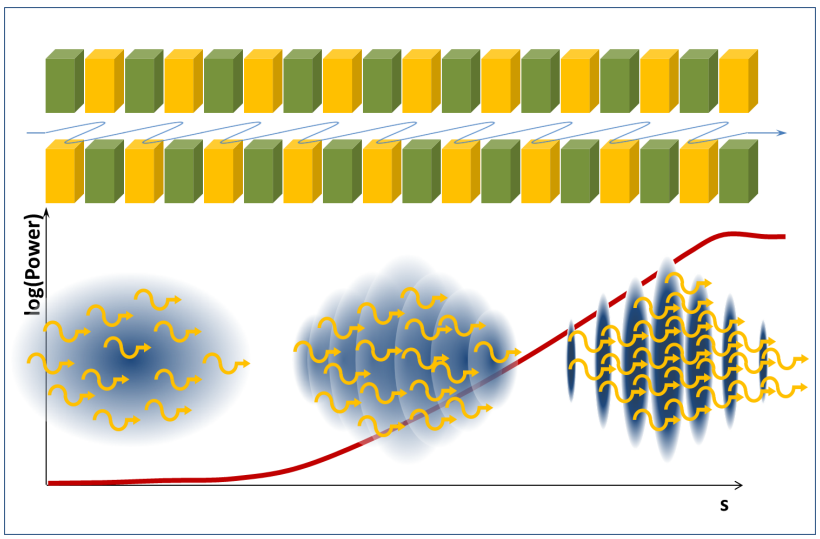

Figure 1: SASE process. Top picture shows the undulator with alternating polarity of magnetic dipoles. As electrons go through the undulator, microbunching occurs (bottom picture). Red line shows the corresponding laser intensity growth (on logarithmic scale). Figure is adopted from [2]

.

The physical process that governs the function of a free electron laser is Self-Amplified Spontaneous Emission (SASE) [3]. The electron beam is injected into the undulator and travels down its length. In the magnetic field electrons are forced to oscillate and radiate energy. The emitted photons propagate slightly faster than the electrons, but interact with them each undulator period. Electrons lose or gain energy depending on the phase, so faster electrons pick up slower ones. The electron density becomes modulated with the wavelength of the radiation field and is divided into microbunches spaced at the laser wavelength (Figure 1). Then, instead of emitting their radiation at random, electrons radiate in phase with the laser beam. This enhances the coherent emission further, which in turn enhances the micro-bunching and amplifies the radiation field. The growth of the radiation mode's strength is exponential until the process saturates. Saturation occurs when the number of trapped electrons losing energy to the wave is balanced by the electrons gaining energy from the wave.

1.2 Terahertz

FLASH is the Free-Electron LASer at DESY that works on the described principle. FLASH1 hall offers five beamlines, one of them being the BL3 which allows a combination of XUV pulses with THz pulses for pump-probe experiments. The THz pulses are generated by a specially constructed undulator implemented in series to the XUV undulators.

THz is conventionally considered to be in the range of 0.1 to 30 THz, which is also called the far-infrared region. A characteristic that gives the THz region its significance is the low photon energy range associated with it. Hence, THz photon energy is not high enough to induce electronic transitions in the solid material that is probed. It only excites the electrons close to the Fermi level, which contribute primarily to the electrical conductivity of the material.

Transmitted through materials it can be used for material characterization, layer inspection, and since it does not ionize easily and is non-destructive, as an alternative to X-rays for producing high resolution images of the interior of solid objects. A number of materials that are opaque to visible light are transparent to the THz radiation, which, combined with its low photon energy, makes it suitable for imaging.

2 Mirror mount stability measurements

2.1 Introduction

In large experimental setups, especially the ones involving X-ray lasers that require vacuum chambers, saving space is of importance, hence compact equipment, especially compact optical elements, hold special value. However, in order to produce compact equipment, some properties of the standard models need to be modified and some features might be lost in the process. The experiment of XUV - THz pump probe that was done at THz beamline at FLASH, required compact mirror mounts.

Our goal was to test the new Standa mirror mount model that has knobs on top, instead of on the side like standard models, which makes it more compact. There is a concern that because of the spring construction of that mirror mount, the knobs are unreliable and can cause it to be unstable

	Thorlabs KS3	Thorlabs Polaris K3S4	Standa 5KVDOM-3
Picture			
Price	175 €	455 €	400 - 500 €

Table 1: Pictures and the prices for tested mirror mounts. Pictures are adopted from [4], [5], [6]

and to drift. In this part of the project we conducted several types of measurements to determine whether it is stable enough to be used in experiments.

We tested the following models of mirror mounts

- Thorlabs KS3, [4]
- Thorlabs Polaris K3S4, [5]
- Standa 5KVDOM-3, [6]

(We will address them as Thorlabs, Polaris and Standa). They all have three inch optical diameter, and two knob adjusters. Their pictures and prices are shown in the Table 1.

Our idea for measuring stability of mirror mounts was to shoot the laser light onto a mirror and observe the movement of the reflected beam. In order to detect the angular movement of the mirror with better precision we needed the laser path to be as long as possible. Since we had limited space on the optical table (1m), the idea was to use two mirrors in order to get several reflections. More importantly, small jitter of the mirror is magnified by multiple reflections.

2.2 Experimental setup

The experimental setup with indicated elements is shown on Figure 2. The distance between tested and reference mirror is 1m. We used Thorlabs CPS635R laser of 635 nm wavelength, 1.5 mW power. The laser light goes through the polarizer, therefore we can control the intensity that falls on the camera. After that it is directed onto two alignment mirrors, in order to control its position on the tested mirror. Four reflections were achieved on each mirror. We used Thorlabs KS3 mirror mount for the reference mirror. We film the laser beam profile with the digital camera (Thorlabs US82.0), that is positioned behind the tested mirror and catches the fifth reflection. Pixel size of the camera is 4.65 μm, representing the resolution of the beam movement.

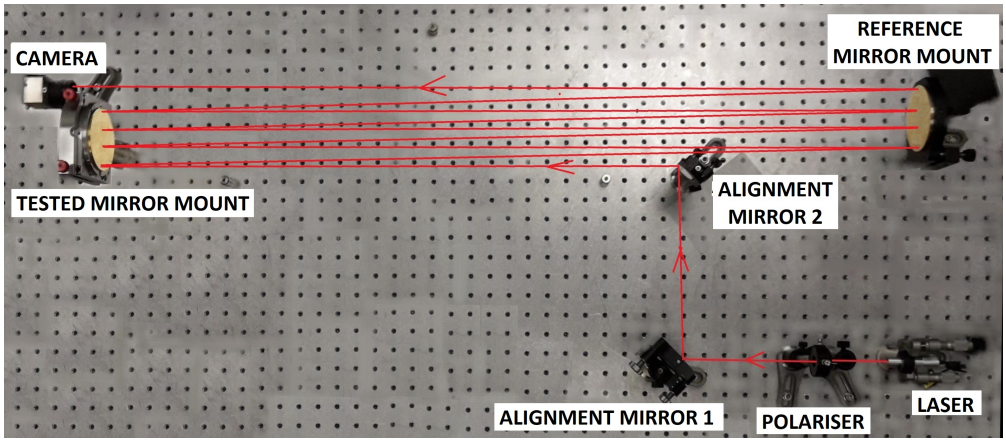

Figure 2: Experimental setup. The red line represents the laser path.

2.3 Image processing

In order to find the center of the beam from the picture of its profile, we used image moment. Image moment of order (i, j) is given by the equation

$$M_{ij} = \sum_x \sum_y x^i y^j I(x, y)\,, \tag{1}$$

where x and y are coordinates of the certain pixel, and $I(x, y)$ is its intensity. The sums go over the entire range of the picture. Center of the laser beam is determined by the center of image moment value, which is given by

$$(x_c, y_c) = \left(\frac{M_{10}}{M_{00}}, \frac{M_{01}}{M_{00}} \right). \tag{2}$$

In principle, it comes down to calculating the center of mass, but with pixel intensity as a weighting parameter.

We extracted only red color data from RGB picture (since our laser is red), and normalized each frame in order to bring them to the same value range of 0 - 1. An example of a processed image is given in the Figure 3. The red circle corresponds to calculated center of the beam.

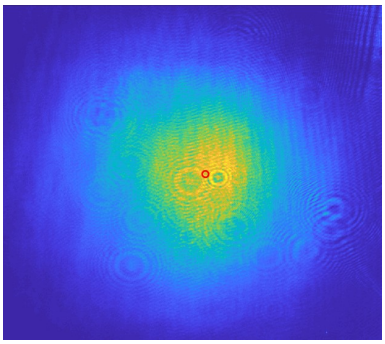

Figure 3: An example of a processed image. The red circle represents the calculated center of the beam

2.4 Results and data analysis

We did three sets of measurements for each mirror mount:

- short-time measurements (during 1 minute)
- long-time measurements (during 2-3 hours)
- knob reliability measurements

Firstly, we excluded influence of the air flow and instability of the optical table, by inducing bigger distortions. The results during distortions didn't show significant difference. On the other hand, we had problems with the intensity of the laser light and its stability. For some time after turning it on, the intensity would drop or rise in an unpredictable way. That would induce changes in the shape of beam profile and hence the error in calculation of the center of the beam, with the method that we use.

2.4.1 Short-time measurements

In Figure 4 we show the center position of the laser beam over time, for each mirror mount (approximately one minute long measurements). Blue line shows the x coordinate of the laser beam, and green line shows the y coordinate. Their standard deviations (STD) are presented in the legends. It can bee noticed that the standard deviation for y coordinate is always bigger than for x coordinate, which indicates that the system is more unstable along the y axis.

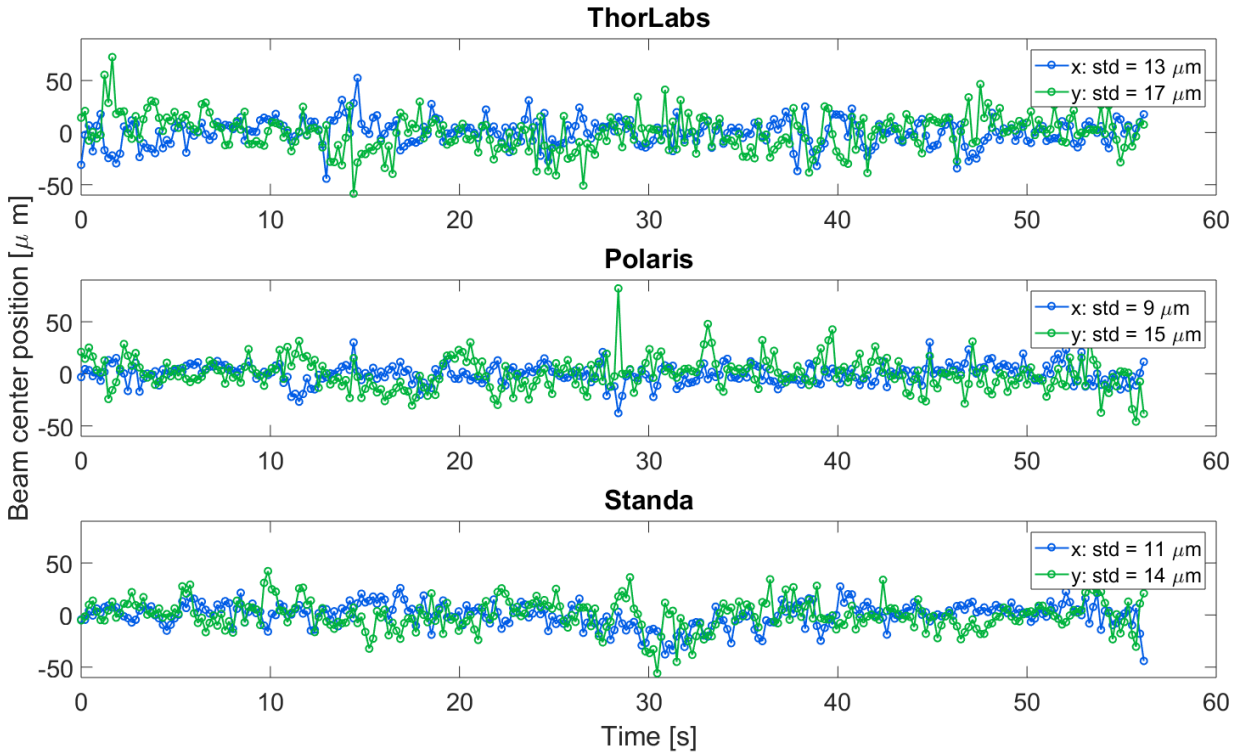

Figure 4: Position of the center of the beam for 1 minute measurements. Blue line corresponds to x coordinate, and green line represents y coordinate. Standard deviations are indicated in the legends

We did 9 measurements for each mirror mount, with different initial settings, for example some are after turning the knobs, and some after being still for a few hours. This measurements didn't show a significant difference in standard deviation, so we averaged all of the data, and the standard deviations are shown in the Table 2. We can see that they are really close in values, hence we

cannot make conclusions about the stability of each. Instead, we suspect that it is a consequence of instability of the laser itself.

Table 2: Standard deviations of beam center position for one minute measurements

	Thorlabs	Polaris	Standa
x STD [μm]	15	16	19
y STD [μm]	30	27	25

2.4.2 Long-time measurements

Because of the fact that the short-time measurements didn't give us useful comparison between the tested mirror mounts, we did long-time measurements. The camera was taking one picture each minute for 3 hours. The recordings are done after inducing small distortions (by turning the knobs, or poking the mirror mounts). The results are shown in the Figure 5. (Note that the y axis range is not the same for the x and y coordinate.) It is noticeable that there are some shifts of the laser beam at the beginning of the measurement, but after some time (around 100 min) it stabilizes. Thorlabs and Polaris mirror mount have comparable standard deviations for both x and y beam center coordinate. However, Standa mirror mount has much smaller x STD and much bigger y STD. It is very stable along the x axis from the very beginning of the measurement, but it shows significant shift along the y axis.

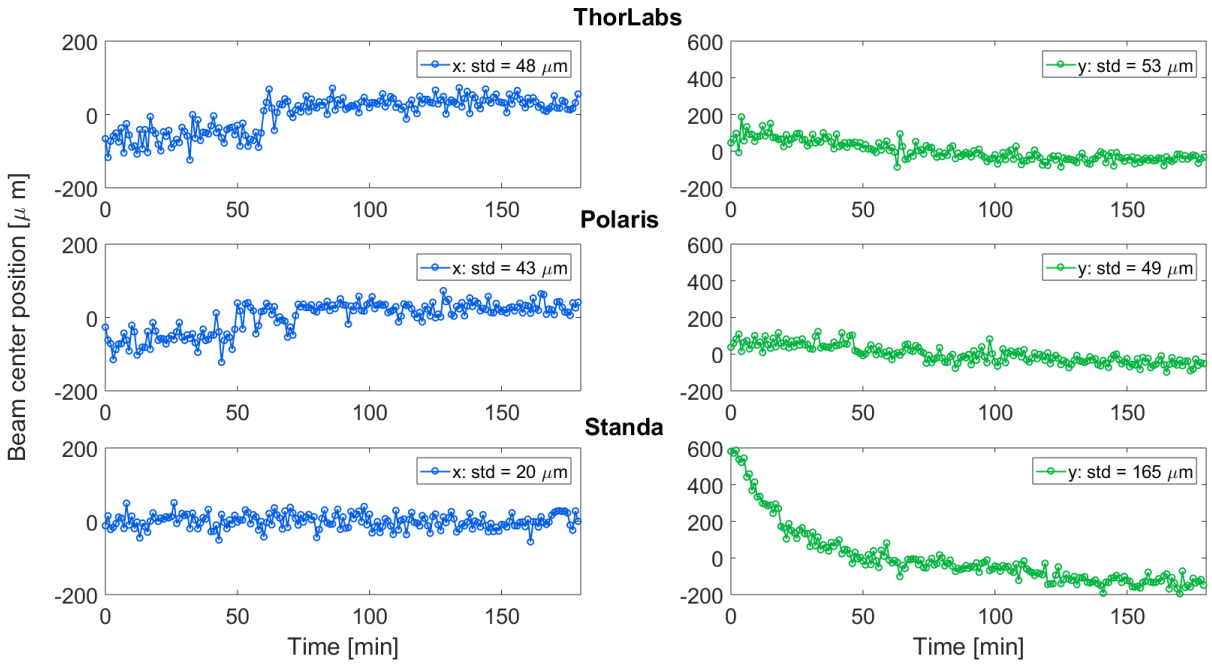

Figure 5: Position of the center of the beam for 3 hour measurements taken after inducing small distortions. Blue line corresponds to x coordinate, and green line represents y coordinate. Standard deviations are indicated in the legends.

After 24h another 2 hour long recording was done for each mirror mount. The results are shown in the Figure 6. All three mirror mounts show similar values of standard deviation (on the order of $20-30\,\mu$m). For Standa mirror mount, there were still some bigger displacements present along both axis. Polaris is showing the best performance for stability during two hours. Standard deviation for x coordinate is influenced by first few minutes of measurement, for which the axis is showing non-continuous behaviour (not shown on the graph). We suspect that is is a consequence of laser light instability, which dramatically dropped in that region.

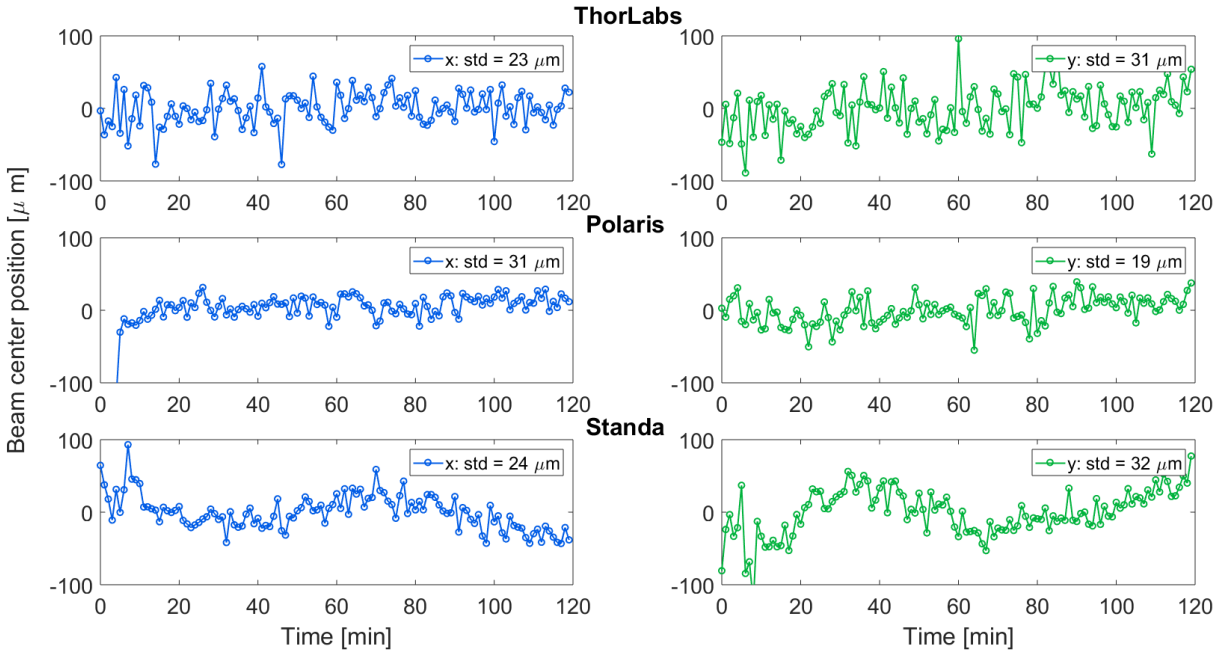

Figure 6: Position of the center of the beam for 2 hour measurements taken after 24 hours. Blue line corresponds to x coordinate, and green line represents y coordinate. Standard deviations are indicated in the legends.

2.4.3 Knob shift measurements

When adjusting the reflected laser light on camera using the knobs of mirror mounts, we noticed that their motion is not completely independent. Namely, when moving the knob that is corresponding to one axis, the laser light also moved along the other axis. To check the reliability of each mirror mount knob, we turned one of the knobs enough for the laser to be off the camera screen, and then roughly back to its original position. We then calculated the shift of the center of the laser along the other axis (that does not correspond to the turned knob). The results are shown in the Table 3.

We can notice that the ThorLabs shows the best performance in testing this feature. Polaris has a bigger drift for x axis than for y axis. Standa mirror mount has significantly larger shifts than the two other mirror mounts. Also, it is noticeable that there is a great difference between the displacements for different direction of turning. For Polaris mirror mount clockwise motion is

Table 3: Displacements of the center of the laser that occur along one axis when the other axis knob is moved

drift	Thorlabs		Polaris		Standa	
	$\Delta x[\mu\text{m}]$	$\Delta y[\mu\text{m}]$	$\Delta x[\mu\text{m}]$	$\Delta y[\mu\text{m}]$	$\Delta x[\mu\text{m}]$	$\Delta y[\mu\text{m}]$
y anti-clockwise	40		131		22	
y clockwise	2		1		141	
x anti-clockwise		10		10		144
x clockwise		20		1		287

more favourable, while for the Standa it is an anticlockwise motion. Thorlabs has different results for different axes. It's worth noting that the turning the knobs by hand is not an adequate way for a controlled and reproducible measurement of this feature, but it gives a rough picture on the correlation of their turning.

2.5 Discussion

When conducting the measurements we had big problems with the laser light stability. The laser intensity would drop and rise unpredictably, and we noticed that there is a jump in x coordinate of the center of the beam, at the same time intervals where the intensity changes (y coordinate is continuous, because the fringes are vertical). On Figure 7 we show one example of such sudden change in intensity. We didn't find the way to avoid this problem in image processing.

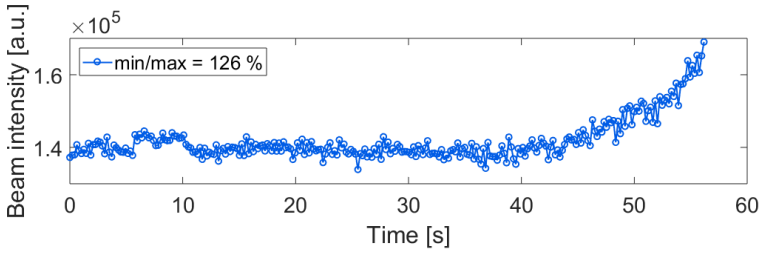

Figure 7: An example of sudden change of intensity of the laser beam over time

Also, laser beam profile wasn't homogeneous, often there were interference fringes present, as can be seen on figure 8a. If the laser beam moves slightly towards the region of camera where there is an interference fringe, its intensity on that fringe would rise more than on the other parts of the beam. Therefore, because of the center of the image method that we are using in image processing, center coordinates would be biased towards the fringe (Figure 8b), and it would show bigger shifts than actually happened. We suggest using better laser and/or camera for more homogeneous and stable beam profile image.

2.6 Conclusion

For a conclusion on these measurements, we can say that all three mirror mounts have similar characteristics considering stability during short-time measurements ($\sim$ 1 min). For the long

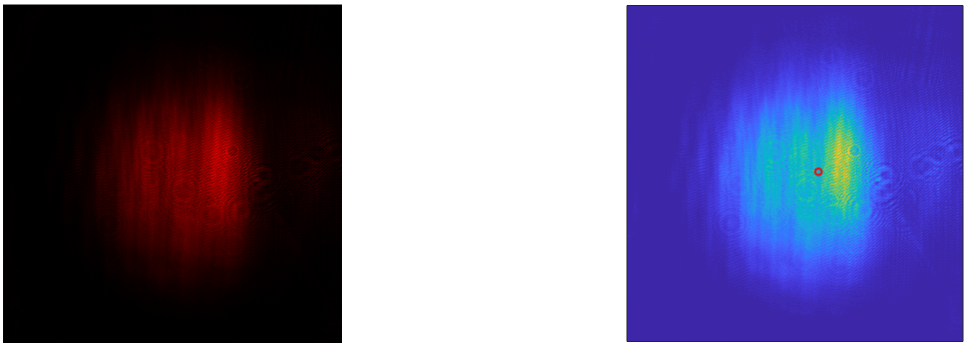

(a) **(b)**

Figure 8: An actual image of the laser beam that shows vertical fringes on the left, and processed image with calculated center (red circle) on the right.

time measurements, we noticed that they have roughly the same stabilization time, but they shift by a different amounts during that period. Namely, Standa mirror mount showed the biggest displacements. After 24 hours of being still, Polaris mirror mount shows the best results. Standa mirror mount shows greater oscillations around a center position along both axes. Considering the knobs reliability, Standa mirror mount has greatest dependency between knob movement. Therefore, it may be harder for control during the alignment processes.

3 Data analysis for THz-XUV pump-probe experiment at FLASH

3.1 Introduction

To measure events happening in femtoseconds or picoseconds, the so-called pump-and-probe technique is often utilized. Two short pulses are required: the pump pulse starts the reaction, while the probe pulse investigates the state of the system after a defined time delay. This experiment is repeated several times with increasing time delays.

The THz beamline at FLASH has been designed to provide coherent femtosecond – picosecond THz pulses. The design of the beamline allows overlapping femtosecond XUV pulses and THz pulses generated by the same electron bunch at the end of BL3. The pulses should therefore be naturally synchronized down to 5 femtoseconds [9].

However, a problem arises when THz and X-ray optical paths are significantly different. Folding of the THz beam creates additional optical path, leading up to a delay of 21.5 ns (roughly 6.5 m of optical path) with respect to X-ray pulses. By introducing an additional optical path for the XUV, the temporal overlap of THz and XUV can be ensured. It is done by utilizing the back-reflection geometry with normal-incidence multilayer mirrors specially designed for a particular wavelength. Two major drawbacks for this technique are low reflectivity and narrow spectral range of the XUV mirrors. The difference in optical path between THz and XUV also causes a large focal size of the XUV beam.

An alternative approach which avoids the need of introducing a delay for the X-ray pulses [8], is to generate double electron bunches, separated by 21.5 ns. The first electron bunch is then used to

generate THz and the second to generate soft X-ray pulses.

The experiment during beamtime at FLASH1 THz beamline was done with a refocusing mirror (back-reflection geometry) technique in order to test the setup before introducing the THz doubler scheme. The experiment was a pump-probe experiment using silicon as a sample. The idea was to use XUV laser as a pump that creates free electrons in silicon, which then becomes reflective for the THz frequencies below the frequency of the induced plasma.

Silicon sample was pumped with THz at two different wavelengths, and for each a different duration of the transmission change effect was observed. Since the change in transmission depends on the arrival time of XUV and THz, it is possible to determine the relative time between two pulses.

3.2 Data analysis and results

The team of the THz beamline recorded transmitted and reflected signal of the silicone sample, for different time delays between THz and XUV pulses. An example of one such recording is given on Figure 9a, where each line corresponds to a signal at a certain delay time. They recorded for 10-20 laser pulses at each delay time. The time of relaxation of the sample is shorter than the time between two laser pulses, so it is considered that the system is in the ground state each time it is shot with XUV pulse that excites it. The data is averaged over these data points, and an example of the averaged transmitted signal is given on the Figure 9b (the reflected signal looks similar). Because we want to extract information about the intensity of the signal with the lowest possible noise, we integrate every signal only between the red lines, that contain most of the signal (they are indicated in the Figure). The section that is integrated is the same for one data set, but we changed it depending on the signal position, for different data sets.

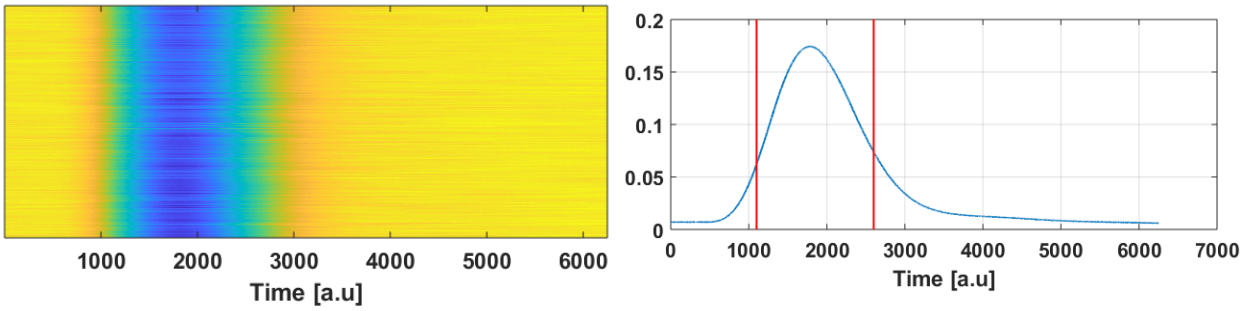

(a) (b)

Figure 9: Complete data set of transparency signal on the left. Each line represents a signal for certain delay time between THz and XUV. Averaged signal over several data points on the right. The red lines indicate the region of integration.

The plot of the calculated intensity parameter for each delay time is shown on the Figure **??**, for transmitted signal on the left and for reflected on the right. Observed parameter is their difference divided by their sum, $\frac{I_R - I_T}{I_R + I_T}$, where I_R and I_T are intensities of the reflected and transmitted signal, correspondingly. We observe the difference because they expect reflected signal to increase, and transmitted to decrease accordingly, so the effect would be more obvious. We divided it by their

sum, to compensate for possible intensity fluctuations of the THz laser before it hits the sample. We also observe the correlation between the reflected and transmitted intensities.

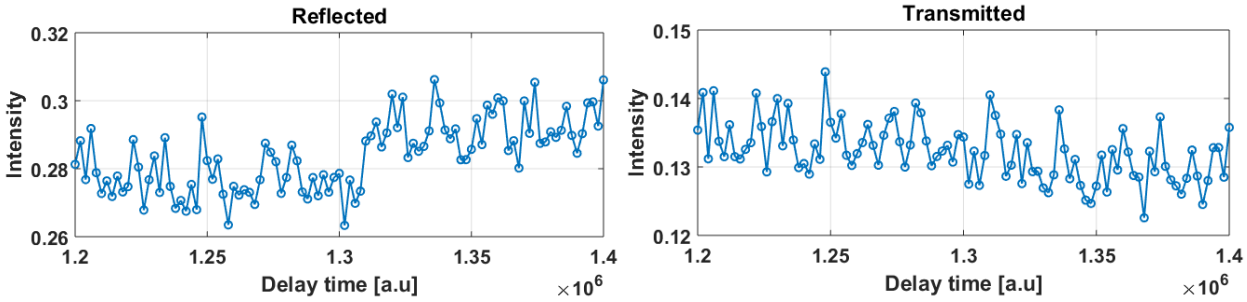

Figure 10: Reflection and transmission intensity after integration of the signals versus delay time between THz and XUV

On Figure **??** we show two sets of data. On top picture there is no visible "jump" of the signal, and the correlation between reflected and transmitted signal is linear, with correlation coefficient value close to 1 (it's indicated in the plot legend). On the other hand, on bottom picture there is a clear jump of the signal, which is also followed by the splitting of the correlation line. These two data sets are conducted using different filters for THz and XUV lasers.

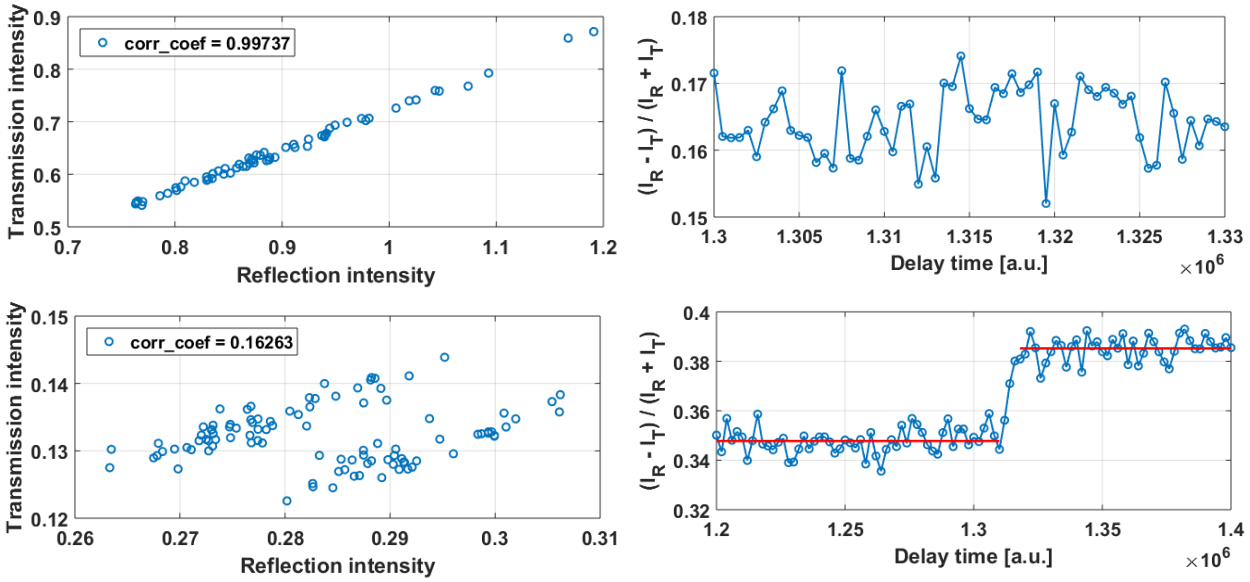

Figure 11: Two sets of data for different filters in the beamline (top and bottom). Correlation of the reflected and transmitted signal is shown on the left and their difference over sum is shown on the right.

3.3 Discussion

It's worth noting that we did data analysis of the results only during three beamtimes at THz beamline at FLASH which was only the first part of the experiment, and we will not be present for the experiment utilizing the THz doubler scheme. Therefore, we didn't conduct further analysis and discussion of the results, since the measurements are not yet complete and published. Our work provided useful information for the choice of the scanning parameters, as the scanning consumes time and the use of FLASH is time-limited for each experiment.

4 2D scanning for THz TDS system

4.1 Introduction

The terahertz time-domain spectroscopy (THz TDS) is a technique for material probing and characterization, based on electro-optic sampling [**?**]. It is based on direct time-domain sampling with an ultrafast laser. Contrary to other spectroscopies, amplitude and phase information are directly retrieved in a single scan, making THz TDS a powerful tool for studying absorption and gain dynamics in semiconductors. Another important advantage of THz-TDS is its high time resolution, which is in the range of 10 femtoseconds or higher, being shorter than the average electron-electron scattering time in semiconductors, and as such, useful in analyzing the dynamics of various processes. It can also be applied in identifying materials owing their unique spectral signature in THz domain.

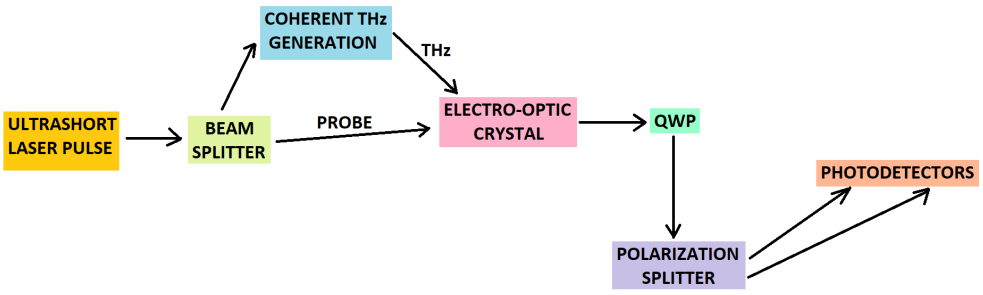

Figure 12: THz time domain spectroscopy (TDS) system scheme

The basic setup of the TDS system, that is shown in Figure 12, contains an ultrashort laser source and a beam splitter that splits each pulse into two. One is then used to generate a coherent THz beam, and the other is used as a probe. These two beams take different optical paths and meet up in the electro-optical crystal. The electric field of the THz pulse acts as an quasi-statical external field that induces changes in the refractive indices along different axes of the electro-optical crystal. So when the linearly polarized probe laser beam passes through and overlaps with it, its polarization is changed, i.e. phase retardation occurs between the two components of its electric field. This process is called linear electro-optic effect or Pockels effect.

A quarter-wave plate (QWP) induces a phase difference of $\pi/2$, hence it can be used to convert linear polarization into a circular one. Since the probe laser experiences a phase retardation in the electro-optic crystal, by installing a QWP after the crystal the final polarization of the probe

becomes elliptical. The beam is then directed to a polarization splitter, which divides the elliptically polarized beam into two orthogonally polarized components. The intensity of those two components are then measured simultaneously with photodetectors. The difference of intensities is proportional to the THz electric field[[10]].

A delay between THz and the probe can be induced using a translation stage, before they are superimposed in the electro-optic crystal. In that way the shape of the THz time domain profile can be recreated.

4.2 2D scanning tool

When having a non-homogeneous sample, it is useful to have an ability to change the focus location on the sample. The idea is set up two stages perpendicular to each other, and attach the sample to it. In that way, 2D scanning of the sample in vertical plane is possible. We wrote a LabView script that controls the movement of all three stages (two for sample scanning and one for inducing time delay). For each position of a 2D stage, the program makes one time delay scan.

4.3 Results

To test the validity of the program we inserted a metal plate with holes, since THz is absorbed in metal. The experimental setup of the stages and attached metal plate can be seen in Figure 13. In Figure 14 we show the picture of the metal plate on the left, and its reconstructed shape from THz imaging on the right. The matching of the images indicated that the program works well.

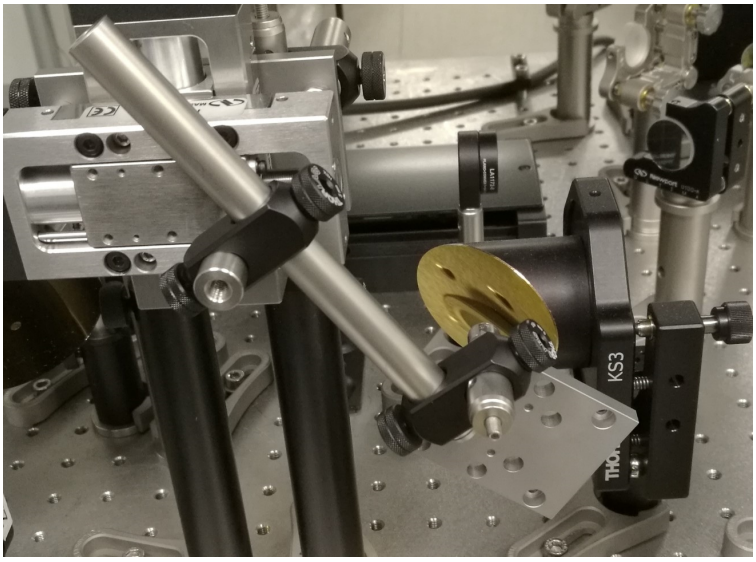

Figure 13: Metal plate attached to the 2D scanning stage and installed in the focus of the TDS system

Using a pinhole in the place of the sample we conducted scanning of the THz beam profile. THz time domain profile is given in the Figure **??**. It is a rough scan along time delay, because scanning process consumes a lot of time. In Figure **??** we show the 2D THz beam profile at delay time $t = 8$ a.u., while in Figure **??** we show 2D scan where for each point of the profile we take the maximum

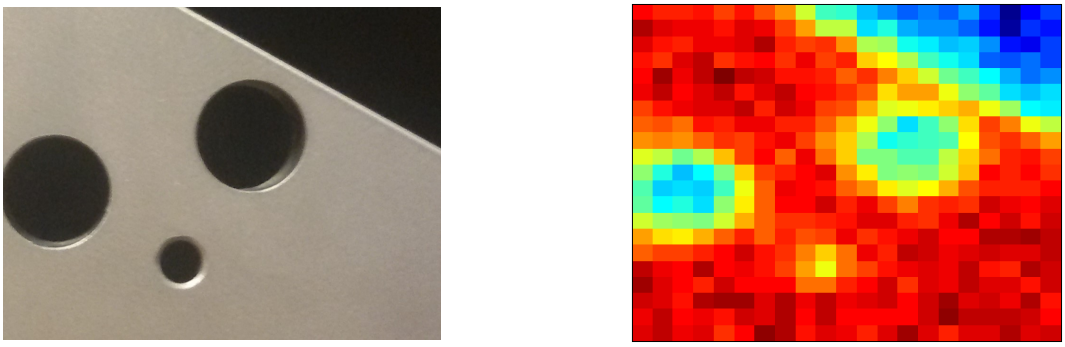

Figure 14: The actual picture of the metal plate on the left and the reconstructed picture from THz imaging, when using metal plate as a sample, on the right

value of THz intensity (along time delay scan). It can be noticed that on the left picture THz beam profile is circular, while on the right picture it is elongated. This indicates that not all parts of the beam arrive at the same time in the focal point. The reason for that is the slight alignment of one of the optical elements, possibly a parabolic mirror that focuses the beam on the sample.

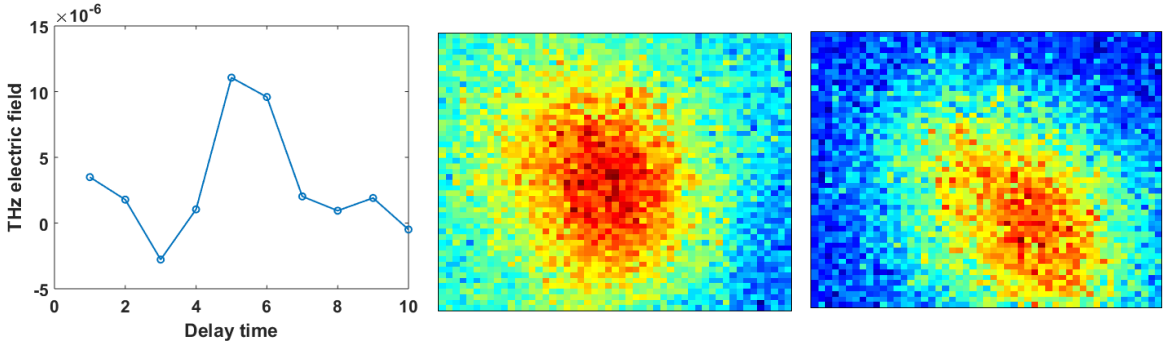

Figure 15: From left to right: THz time domain profile at the center of the beam, THz 2D cros-section profile for fixed delay time at $t = 8$ a.u., 2D cros-section profile with maximum THz signal at each point

The only flaw of the scanning process is that it consumes a lot of time. But on the other hand, the output can give a lot of information about both the sample and THz beam profile. Therefore, we hope that it will be a useful tool in the future experiments.

5 Acknowledgements

We would like to thank Rui Pan for dedicated support and guidance. Special thanks to Nikola Stojanovic and Ekaterina Zapolnova for always offering useful advice and encouragement. We are also grateful to the FLASH team and DESY for giving us the opportunity gain useful experience by participating in the beamtime experiments.

References

[1] Charles A. Brau (1988). *Free-Electron Lasers*, Science, 239 (4844), 1115-1121

[2] Helmholtz Zentrum Berlin: `https://www.helmholtz-berlin.de/projects/berlinpro/erl-intro/linac-fel_en.html`, last visit: 01.09.2018.

[3] A. Lindblad, S. Svensson, K. Tiedtke (2011). *A compendium on beam transport and beam diagnostic methods for Free Electron Lasers*, Deutsches Elektronen-Synchrotron DESY

[4] Thorlabs, Inc: `https://www.thorlabs.de/thorproduct.cfm?partnumber=KS3#ad-image-0`, last visit: 04.09.2018.

[5] Thorlabs, Inc: `https://www.thorlabs.com/thorproduct.cfm?partnumber=POLARIS-K3S4`, last visit: 04.09.2018.

[6] Standa: `http://www.standa.lt/products/catalog/optical_positioners?item=350`, last visit: 04.09.2018.

[7] E. Zapolnova et al. (2018). *THz pulse doubler at FLASH: double pulses for pump–probe experiments at X-ray FELs*, J. Synchrotron Rad. 25, 39-43

[8] Grimm, O., Schreiber, S. & Klose, K. (2006). *Proceedings of the 10th European Particle Accelerator Conference*, Edinburgh, UK, 26–30 June 2006. THPCH150.

[9] Ramesh Arathi, *Optimisation of Terahertz Time-Domain Spectroscopy based on a Photoconductive Antenna*, unpublished bachelor's thesis

[10] Wai Lam Chan, Jason Deibel and Daniel M Mittleman (2007). *Imaging with terahertz radiation*, Rep. Prog. Phys. 70 (2007) 1325–1379